



Baseline Biomechanical Properties of Epithelia prior to Tissue Expansion in Dogs

Jay Bowling, DDS, MSD*†
 Darrell D. Davidson, MD, PhD‡§
 Sunil S. Tholpady, MD, PhD¶
 Kinam Park, PhD§||
 George J. Eckert, MAS**
 Terrence Katona, DO††
 Tien-Min G. Chu, DDS, PhD‡‡
 Clark T. Barco, DDS, MS*

Background: Soft-tissue deficiencies pose a challenge in a variety of disease processes when the end result is exposure of underlying tissue. Although multiple surgical techniques exist, the transposition of tissue from one location to another can cause donor-site morbidity, long incisions prone to dehiscence, and poor patient outcomes as a result. Use of tissue expansion prior to grafting procedures has been shown to have success in increasing available soft tissue to aid in repairing wounds. However, the current tissue expanders have biomechanical limits to the extent and rate of expansion that usually exceeds the tissue capacity, leading to incisional dehiscence or expander extrusion. Understanding the baseline biomechanical properties of the tissue to be expanded would provide useful information regarding surgical protocol employed for a given anatomical location. Therefore, the aim of this study was to test and compare the baseline (pre-expansion) biomechanical properties of different common expansion sites in dogs.

Methods: Four samples measuring approximately 20×15×1 mm were harvested from 8 dogs. The samples were collected from the hard palate, alveolar mucosa, scalp, and chest of the animal and analyzed for stress, strain, maximum tangential stiffness, maximum tangential modulus, and tensile strength using a Texture Technologies TA.XT texture analyzer with corresponding biomechanical measurement software. Samples were compared as to their baseline biomechanical properties prior to any soft-tissue expansion. Histological sections of the samples were analyzed using hematoxylin eosin in an attempt to correlate the histological description to the biomechanical properties seen during testing. Summary statistics (mean, standard deviation, standard error, range) are reported for stress, strain, maximum tangential stiffness, maximum tangential modulus, and tensile strength and for the histological parameters by intraoral site. Analysis of variance was used to compare the biomechanical and histological parameters among the 4 locations while accounting for multiple measurements from each dog.

Results: The scalp had significantly higher maximum stress (σ_{max}) than chest, mucosa, and palate ($P < 0.0001$), with no differences among the other 3 locations ($P > 0.63$). Scalp site also had significantly higher maximum tangential modulus (ϵ) than chest, mucosa, and palate ($P < 0.006$), with no differences among the other 3 locations ($P > 0.17$). The locations did not have significantly different maximum tangential stiffness (k ; $P = 0.72$). Histologically, 2 separate patterns of collagen disruption were evident.

Conclusion: Although different results were obtained than theorized, this study showed that the scalp had the greatest resiliency to expand prior to tearing, and the highest tangential modulus, with all sites having statistically similar modulus of elasticity. Based on this study, the scalp could be expanded more aggressively compared with the other sites. (*Plast Reconstr Surg Glob Open* 2018;6:e1773; doi: 10.1097/GOX.0000000000001773; Published online 14 May 2018.)

From the *Roudebush Veteran Affairs Medical Center, Dental Service, Indianapolis, Ind.; †Department of Periodontics, Indiana University School of Dentistry, Indianapolis, Ind.; ‡Department of Pathology and Laboratory Medicine, Indiana University, Indianapolis, Ind.; §Akina, Inc. West Lafayette, Ind.; ¶Roudebush Veteran Affairs Medical Center, Plastic Surgery Division, Indianapolis, Ind.; ||School of Biomedical Engineering, Purdue University, West Lafayette, Ind.; **Department of Biostatistics, Indiana University School of Medicine, Indianapolis, Ind.; ††Roudebush Veteran Affairs Medical Center, Pathology Service, Indianapolis, Ind.; and ‡‡Department of Biomedical and Applied Sciences, Indiana University School of Dentistry, Indianapolis, Ind.

Received for publication July 6, 2017; accepted March 13, 2018. Supported with resources and use of facilities at the Richard L. Roudebush VA Medical Center, Indianapolis, Ind. Resources were also utilized from Indiana University, Indianapolis, Ind., in providing biostatistical funding for the study.

Copyright © 2018 The Authors. Published by Wolters Kluwer Health, Inc. on behalf of The American Society of Plastic Surgeons. This is an open-access article distributed under the terms of the Creative Commons Attribution-Non Commercial-No Derivatives License 4.0 (CCBY-NC-ND), where it is permissible to download and share the work provided it is properly cited. The work cannot be changed in any way or used commercially without permission from the journal. DOI: 10.1097/GOX.0000000000001773

INTRODUCTION

Insufficient viable soft tissue presents a common challenge for a variety of reconstructive surgical procedures, including congenital malformation conversion, traumatic injury repair, cancer extirpation, and restoration after extensive infections. Necessary reconstructive surgery may be complicated by secondary donor-site problems, loss of function, or contour deformities. Ensuring a successful outcome in large wound reconstruction depends on a tension-free (passive) primary closure, which requires large-scale tissue mobilization.^{1,2} Excessive flap deformation, however, can increase the risk of soft-tissue dehiscence, and infection.^{3,4} One of the most versatile and aesthetically available options to create soft tissue for surgical reconstruction is soft-tissue expansion.⁵

Tissue expansion refers to a device that gradually stretches the tissue near a defect induces reparative proliferation and increases the extent of tissue after distension. Balloon-type devices have been widely used to reduce the uncertainty of clinical success with traditional flap procedures or releasing incisions.⁵ Tissue expansion requires gradual internal expansion of skin, fat, and muscle to a shape and size required for recipient-site closure. Studies of tissue expansion have found that the vascularity of the expanded flap is maintained, or even increased because of reparative tissue neovascularization of reproductive tissue.^{6–8}

Biomechanical and circulatory properties of the expanded soft tissue can significantly affect the clinical outcome of reconstructive surgical procedures.^{9,10} Additional tissue is regularly needed for passive primary closure in skin of palate, alveolar mucosa, chest, and scalp. The mechanical capacity of each surgical site to be safely manipulated may vary. Furthermore, sites adjacent to bone loss may require greater expansion to accommodate bone graft and to prevent motion caused by soft-tissue movement.¹¹ One solution for increasing tissue for covering intraoral bone grafts is preprogrammed expansion of the epithelia by osmotic devices.¹² Periosteal releasing incisions may also be successful, but this approach is strictly dependent on the host response and on operator skill with significant reduction in perfusion to the soft tissue (skin or mucosa) overlying a bone graft.¹³

All tissue expansion carries risks of wound dehiscence and infection.¹⁴ Although expansion with balloon-type devices can be controlled, multiple fills are required. Self-expanding osmotic hydrogel devices, on the other hand, are implanted once, the incision closed, and the hydrogel expands on its own. The main limitation of hydrogel tissue expanders is that the rate and extent of expansion are predetermined by the composition of the device and cannot be altered after surgical placement. The biomechanical properties of the surgical site are a key guideline for hydrogel device design. The baseline biomechanical ca-

capacity at common sites for tissue expansion has not been well studied.

Not all tissues expand at the same rate in response to a scheduled force. Overly rapid expansion disrupts tissue and impairs the healing response, often with unwanted complications.^{15,16} It is vital to understand the underlying biomechanical properties of the soft tissue to be expanded to formulate the correct hydrogel tissue expander force and rate of expansion to match each anatomical site.¹⁵

A critical limitation of hydrogel tissue expanders is that the rate and extent of expansion are predetermined by the hydrogel composition and cannot be altered after surgical placement. The underlying biomechanical properties of the tissue to be expanded are a key for all hydrogel tissue expansion design and clinical success. We intended to address important physical characteristics of different soft tissues expanded in routine clinical use, to modify the rate and force of expansion of hydrogels tailored to different anatomical sites—palate, oral mucosa, chest, and scalp—for more successful clinical outcomes. The aim of this study was to test and compare the inherent biomechanical properties of common tissue expansion sites in dogs.

METHODS

Study Design

Thirty-two epithelial samples, measuring 20×15 mm length and width, and approximately 1 mm thickness, were harvested from 8 study dogs. Samples from each dog were collected from 4 sites: the hard palate, alveolar mucosa, chest, and scalp, as shown in Figure 1. The subjects were mixed breed and mixed sex hounds, aged 1–2 years, from a Class A dealer. The animals used for this study were authorized according to the tissue institutional animal care and use committee sharing policy of the Indiana University School of Medicine. Care was taken to harvest periosteum with mucosal and palatal samples and to take only epidermis, reticular dermis, and appropriate connective tissue without excessive fat in the chest and scalp sections. The sample thickness ranged from 0.5 to 1.2 mm as measured by Vernier calipers. The goal was to test the *in vitro* biomechanical properties of samples from different sites for which tissue expansion may be required for wound closure.

Fur was removed with clippers from the scalp and chest before harvesting. The harvested test samples were placed immediately into 0.9% saline at room temperature. Additional control tissue adjacent to each harvest area was taken from 4 animals and placed in 10% neutral buffered formalin for histological analysis. Test strips were fixed immediately after biomechanical property measurement.

Histological Analysis

Both test and control tissue samples were fixed for 8–24 hours in 10% phosphate-buffered formalin at room temperature, then dehydrated and embedded in paraffin blocks according to laboratory standard procedures. Histological sections were deparaffinized and stained with hematoxylin and eosin. Slide preparation and histological

Disclosure: *The authors have no financial interest to declare in relation to the content of this article. The Article Processing Charge was paid for by the Indiana Institute for Medical Research.*

descriptive tissue analysis of the samples were supervised by a certified dermatopathologist at the VA Pathology Service (T.K.).

Biomechanical Test Procedures

Mechanical testing began immediately after tissue harvesting. A Texture Technologies TA.XT texture analyzer (Texture Technologies Corp., Stable Micro Systems, Ltd, Hamilton, Mass.) exerted gradually increasing force to stretch tissues while measuring the tissue resistance to deformation. Each sample was attached to clamps modified to receive tissue strip samples and was subsequently ana-

lyzed with a force to distance traveled plot. Using biometric software program accompanying the testing device, the data were transfigured into an individual sample stress/strain curve (Fig. 2). From the curve, the stress, strain, maximum tangential stiffness (MTS), and maximum tangential modulus (MTM) were calculated. Stress measures the force applied to the tissue per cross-sectional area unit. Strain measures the tensile lengthening of the tissue when that stress is applied. As biological materials undergo tensile stress, they tend to stiffen, resisting further lengthening as the collagen bundles and elastin fibers extend to their maximum natural length. MTS measures the tissue

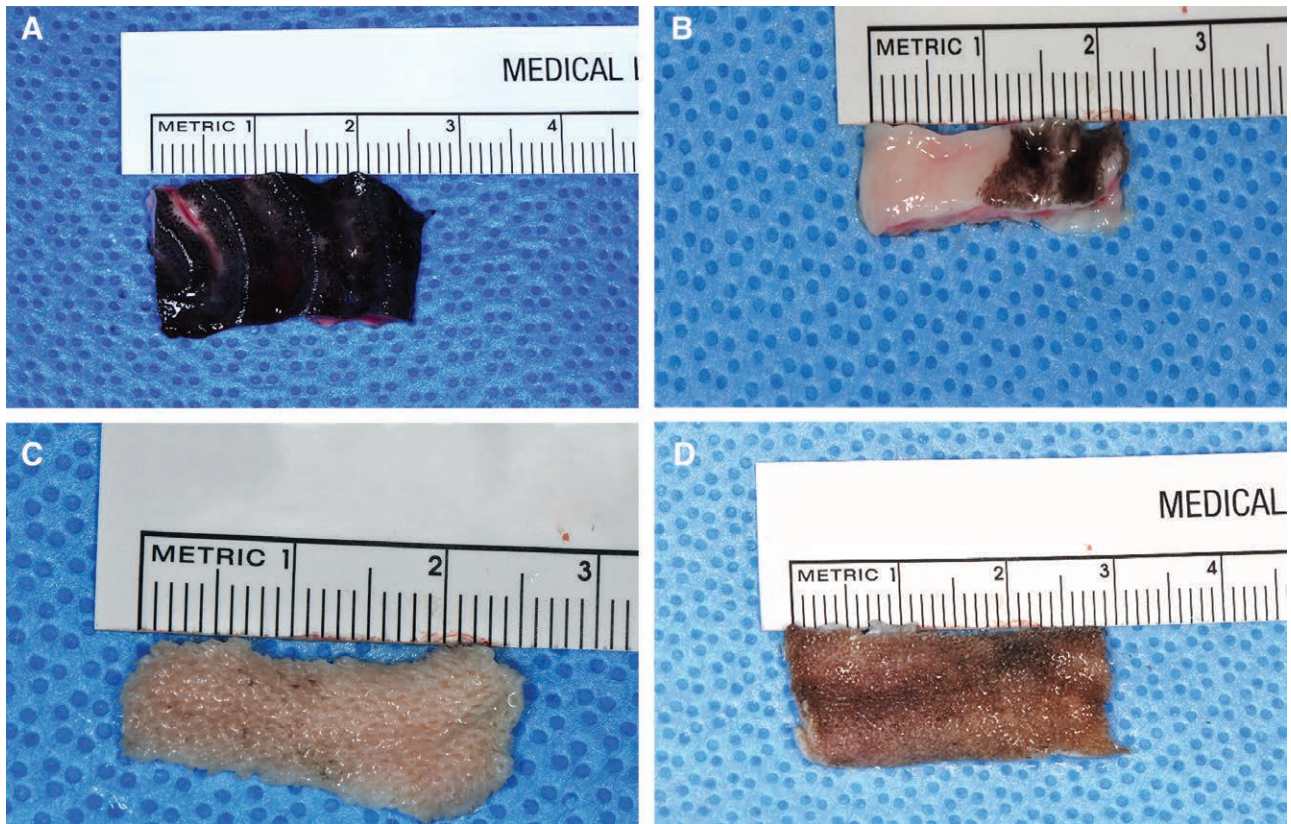


Fig. 1. Harvested samples from sites. A, Palate mucosa, B, Alveolar mucosa. C, chest. D, Scalp.

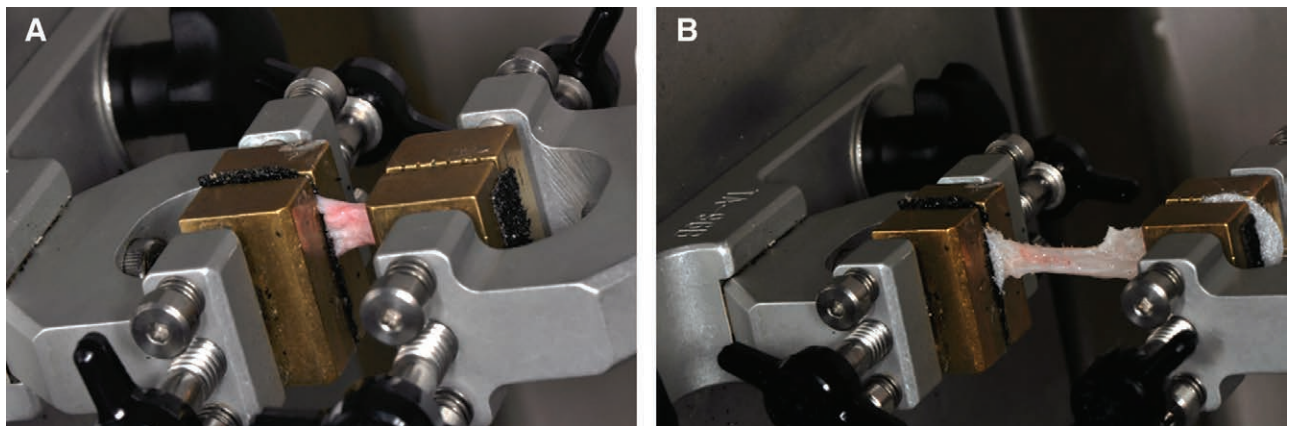


Fig. 2. Diagram illustrating biomechanical testing procedures. A, Pretest loading. B, Posttest loading.

performance under additional lengthening after this elastic region of the stress/strain curve is exceeded. The MTM measures the relationship between stress (force per unit area) and strain (proportional deformation). MTM is a parameter describing the relative elasticity (“stretchiness”) of a material regardless of geometry.

The strip initial length between clamps was measured by the calibrated TA.XT machine. The other strip dimensions (width and thickness) were measured using calipers for calculating the initial cross-sectional area. The mechanical characteristics of each sample were determined under the uniaxial tensile test performed at a constant loading rate of 1 mm/s until rupture, obvious material biomechanical failure, slippage of the sample in the clamps, or a predetermined loading period of 20 seconds. The specimens were kept moist in 0.9% saline solution from harvesting until clamping in the biomechanical measurement instrument.

The measured force and displacement data were transformed into engineering stress (σ) and strain (ϵ). Stress is the applied force (F) in Newtons normalized by the deformed cross-sectional area (A):

$$\sigma = F / A$$

where A (mm^2) is the current cross-sectional area calculated at that length assuming a constant volume of the sample. The stress was calculated with an assumption that the mucoperiosteal tissue is incompressible. The engineering strain (ϵ) was calculated as deformation normalized by the original specimen length:

$$\epsilon = \Delta L / L$$

where L (mm) is the original length of the specimen and ΔL (mm) is the elongation. Standard stress-strain curves were plotted to determine the mechanical parameters of interest. The modulus tensile strength MTM and MTS were calculated for each test specimen.

The MTS is the maximum slope of the force/distance curve from which the stress/strain curve is derived. MTS thus indicates the relationship between force and distance at which the material reaches maximum resistance to further deformation. MTS is dependent on the specimen geometry and may differ based on specimen dimensions. From the stress-strain curve, MTM was derived as the maximum slope of the stress/strain curve corresponding to the linear part of the curve representing the viscoelastic phase of specimen extension (Fig. 3). The MTM is an intrinsic property of the material and is useful to compare tissues from different sites.

Statistical Analysis

The instrument reported force and distance parameters at 2.5 millisecond intervals so a 20-observation moving average was used to smooth the curves before calculating the MTM from the stress-strain curve. Likewise, the MTS was plotted from the force-elongation values using a 20-observation moving average.

A mixed-model analysis of variance was used to compare the 4 locations within each dog. On the basis of a previous study,¹⁷ the SDs for MTS and MTM were expected

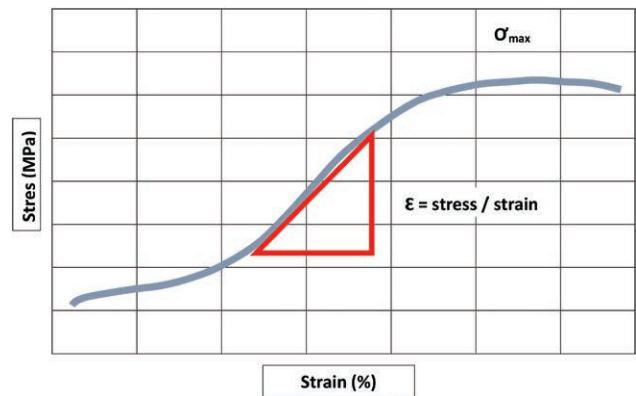


Fig. 3. Sample stress/strain curve and tested biomechanical properties.

Table 1. Results from the Biomechanical Testing

Outcome	Chest	Mucosa	Palate	Scalp
s_{mak}	2.82 (0.78)	2.62 (1.12)	2.78 (1.04)	5.15 (0.81)
E	0.068 (0.020)	0.058 (0.015)	0.079 (0.031)	0.124 (0.043)
k	2,128 (1,176)	2,066 (1,904)	1,518 (1,261)	2,255 (919)

E, modulus of elasticity (units are Pa or N/m^2); k, tangential modulus (units are Pa or N/m^2).

to be 0.27N/mm and 1.1 MPa, respectively. For the calculations, a correlation of 0.5 among the sites was assumed. With a sample size of 8 dogs, the study was designed to have at least 80% power to detect differences between any 2 sites of 0.31N/mm for MTS and 1.3MPa for MTM, assuming 2-sided tests each conducted at a 5% significance level.

RESULTS

Biomechanical Properties

Results from the biomechanical testing are presented in Table 1 and are shown in Figures 4, 5. The scalp had a significantly higher maximum stress (σ_{max}) than chest, gingiva, or palate ($P < 0.0001$), with no differences observed among the latter 3 locations ($P > 0.63$).

The scalp also had a significantly higher MTM than the chest, gingiva, or palate ($P < 0.006$), with no differences observed among the other 3 locations ($P > 0.17$). The results further indicate no significant difference of MTS values among the 4 sites, ($P = 0.72$) possibly due to greater average thickness of the scalp specimens. We compared test and adjacent control stripes from each anatomic site to understand why the scalp should have higher maximum stress, and MTM from the other sites. Because most tests proceeded to rupture or mechanical failure, histology usually showed collagen breaches.

Histological Analysis

The test tissues (stretched samples) showed these breaches in 2 patterns. One pattern was a predominantly linear horizontal split in the dermis parallel to the over-

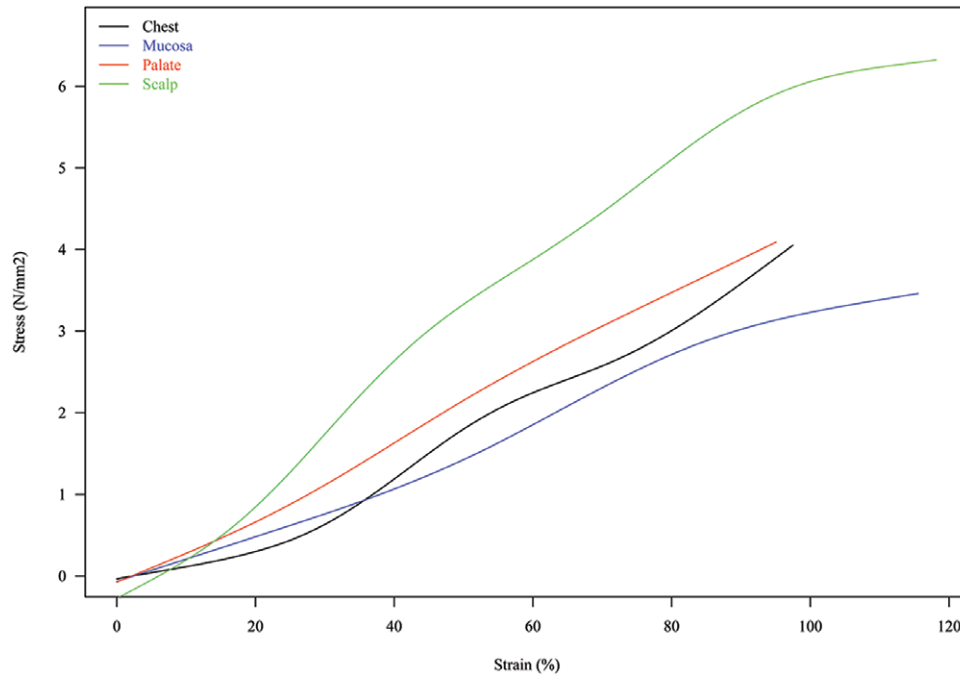


Fig. 4. Results showing the maximum stress, modulus of elasticity, and tangential stiffness of the different sites.

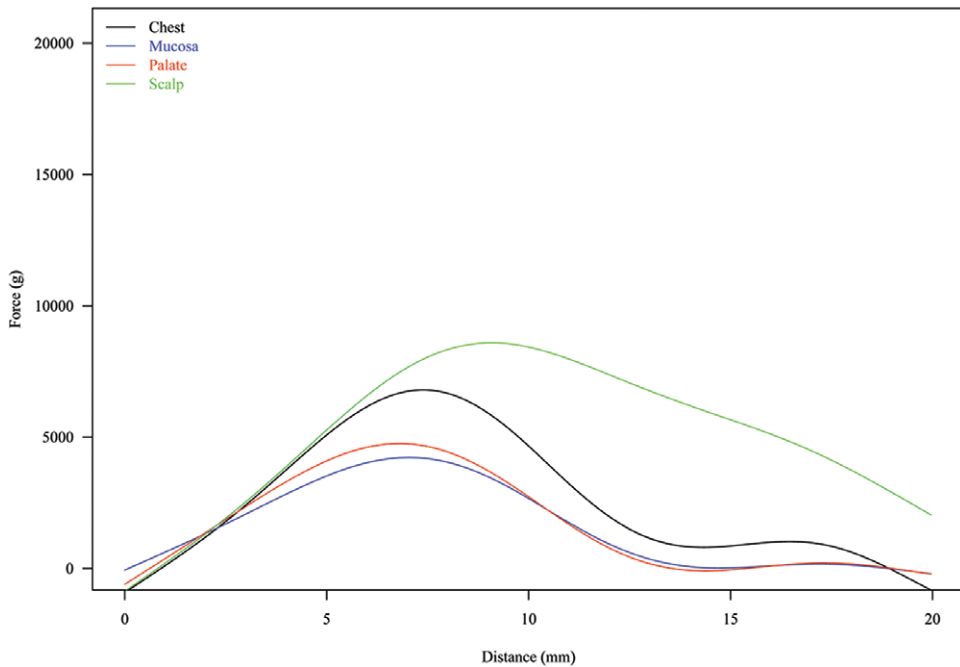


Fig. 5. Results showing the MTM and tangential stiffness of the different sites.

lying epithelium. A second pattern showed smaller areas with the fraying of collagen fibers at random angles relative to the surface. Each site, however, showed variations between dogs in the splitting pattern histologically, possibly based on factors such as sex and nutritional status. Moreover, both splitting patterns were occasionally found in control tissue histology, suggesting that these collagen disruptions were not due to the tissue elongation test.

These complete separations of connective tissue apparently represent an unpredictable artifact use. We, therefore, compared elongated and control tissue detailed micro-anatomy. Palatal mucosa had broad rete ridges, thin collagen bundles in a tiny haphazard arrangement, and both mucinous glands and tiny patches of fat in the deep sub-mucosa. After elongation, the dermal papillae were wider, and collagen bundles were thinner and more horizontally

oriented than in the control submucosa. Mucous glands were lost, and there was extravagated mucin between collagen bundles. Fat cells, in this and each tested tissue, showed breaks in adipocyte cell membranes and a more polygonal rather than rounded cell outline.

Alveolar mucosa had a thin epithelium with expanded superficial epidermal layer. The collagen bundles had the thinnest and most churning appearance of the 4 control tissues. The deep subepithelium contained scant fat, no glands, and scattered skeletal muscle bundles. After elongation, the alveolar collagen bundles of submucosa were closer, more compact, and more often horizontally oriented than in the control slides.

The chest skin had abundant hair and skin adnexa penetrating a thin epidermis containing 20% orthokeratosis. Collagen bundles tended to be thin, widely spaced, and mainly arranged around hair follicles. Elongation caused less alignment of collagen bundles than in palate or scalp. However, the collagen showed homogenization and loss of internal structure with overall increased avidity for the eosin stain hypereosinophilia. This hyalinization and hyper-eosinophilia were hallmark changes in the collagen of test tissue from each of the 4 sites. These collagen bundle changes were generally seen in all 4 sites and were accompanied by loss of space between adjacent bundles.

The scalp skin had abundant hair and a keratin layer about 50% of the epidermal thickness. The collagen bundles of control dermis were delicately random as in alveolar mucosa. The deep dermis contained small islands of fat near hair follicles, but no flat or continuous layer of fat. After elongation of either scalp or chest skin, the hair shafts became more aligned and tilted at a sharper angle. Collagen bundles of scalp dermis, unlike the other sites, appeared to coalesce and become larger. The hyalinization and hyper-eosinophilia of these bundles were more pronounced than at the other sites. Alignment of the dermal collagen bundles along the axis of elongation was greater in the scalp specimens when compared with control tissue collagen alignment than in other sites. These histologic changes are demonstrated in Figure 6.

DISCUSSION

This study aimed to test and compare the baseline biomechanical properties of dog tissue sites likely to need expansion for clinical reconstructive procedures. Few studies have evaluated these important properties of tissues commonly affected by restorative operations. Whether by episodic balloon-type soft-tissue expansion or with continuous osmotic-type expansion, there are limits to the soft-tissue capacity and facility of expansion. When these limits are exceeded, negative outcomes can occur.¹⁷ Rapid epithelial tissue expansion may damage the stem cells and extracellular matrix needed for reparative responses with impaired neovascularization and collagenization. Ulceration may occur increasing the possibility of infection.¹⁴ Maximum stress is attributable to the collagen fibril density, elastin content, and sample tissue thickness and represents the maximum force that should be applied during tissue expansion. The higher maximum stress and MTM

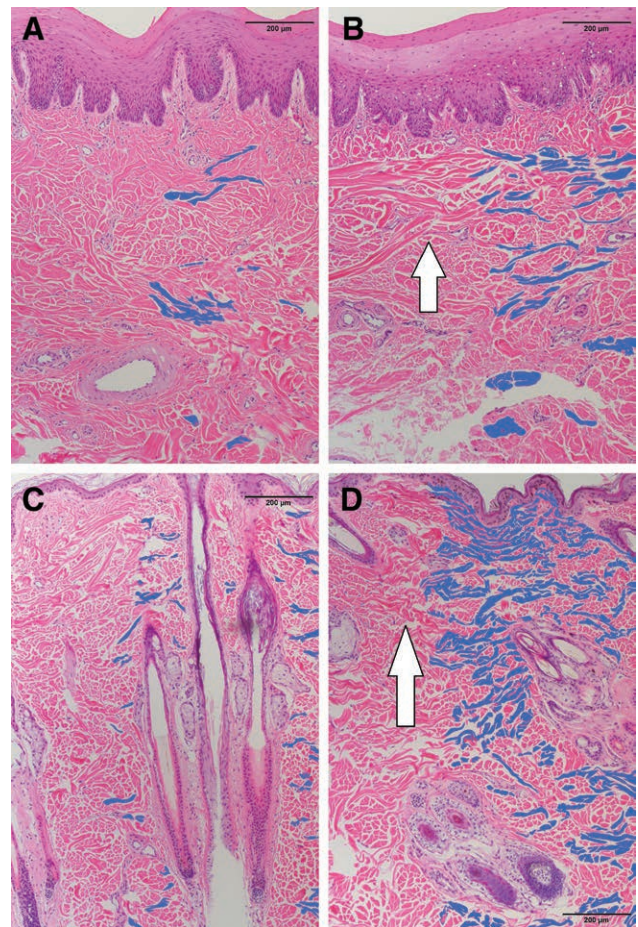


Fig. 6. Histological photomicrographs of samples: A, Palate mucosa control. B, Palate mucosa after stretching. C, Scalp skin. D, Scalp skin after stretching (100 \times). Blue highlighting on the right side of each photograph emphasizes collagen bundles horizontally oriented along the axis of test force. Collagen bundle hypereosinophilia is apparent when comparing the left side of each control and tested tissue photograph (white arrows).

of scalp suggest that this tissue may be expanded more aggressively than other sites.¹⁸

This study measured the biomechanical properties of the tissues before expansion. Additional information regarding fibril density and elastin content may be beneficial in correlating the biomechanical properties of each anatomical site.

Tissue expansion rabbit palatal mucosa showed histological changes consistent with compaction of collagen fibers with an accompanying decrease in tissue thickness and a blurring of tissue layer boundaries.^{19,20} In canine skin, dermal hair follicles provide an additional mechanism for anchoring the epidermis to the underlying dermis.²¹ Therefore, areas with hair, such as chest and scalp, may have an increased ability to stretch compared with hairless areas, such as oral mucosa.

Although care was taken to harvest a consistent sample thickness for MTS comparisons, the thickness ranged from 0.6 to 1.5 mm depending on the site, the dog, and the amount of dermal connective tissue. Samples from the

Table 2. Definitions

Term	Definition
MRE	Measurements of the viscoelastic properties of soft tissue
Maximum stress (σ_{max})	Attributable to the collagen fibril density, elastin content, and sample tissue thickness and represents the maximum force that should be applied during tissue expansion. The higher maximum stress and MTM of scalp suggest that this tissue may be expanded more aggressively than other sites.
MTM	Measures the relationship between stress (force per unit area) and strain (proportional deformation). MTM is a parameter describing the relative elasticity (“stretchiness”) of a material regardless of geometry.
MTS	Measures the tissue performance under additional lengthening after this elastic region of the stress/strain curve is exceeded.
Tangential modulus (ϵ)	Measure of the stiffness of a solid material and defines the relationship between stress (force per unit area) and strain (proportional deformation) in a material, which aid in describing the relative elasticity (or stretch) of a material.
Tangential stiffness (κ)	Similar to tangential modulus, except that it is measuring the reaction of the material to additional tension AFTER the point in which the material is no longer acting in the elastic region of the stress/strain curve, past the point where the material is now permanently deformed.
Tensile strength	Maximum amount of “stretch” before the material is permanently deformed (the object will not return to its original shape or form), and could also represent the point at which the material fails (tears).
Uniaxial tensile test	A popular method of evaluation of mechanical properties of soft tissues in vitro.

palate and alveolar mucosa were relatively easy to obtain, because periosteal stripping determined the deep margin of the specimen. Although similar harvesting techniques were used for the scalp and chest, these samples were much thicker, and no fascial boundary separated dermis from deep connective tissue, such as fat and muscle. We removed grossly apparent fat and muscle before testing for 2 reasons: (1) to test equivalent tissue layers between sites; and (2) to reduce the probability that oily samples would slip from the clamps when being stretched. The impact of the test tissue thickness per site was therefore nonuniform in nature, and likely affected results for MTS evaluations.

The uniaxial tensile test used here is a popular method to evaluate soft-tissue mechanical properties in vitro. The quality of these measurements is highly dependent on the test conditions, the specimen preparation, and sample storage. To obtain reliable measurements, the harvested tissue was immediately tested to minimize autolytic changes.²² An alternate biomechanical property test method would be magnetic resonance electrography (MRE), a powerful tool, as shown by in vivo measurements of the viscoelastic properties of the soft tissue in the oral cavity.²³ Noninvasive MRE measurements, which may safely be obtained from humans, quantitatively measure soft-tissue elasticity in vivo. However, before initiating clinical hydrogel tissue expander studies by MRE, in vitro studies must be completed to determine the biomechanical properties of relevant tissues.

Our results were not as expected. This was possibly due to samples prematurely slipping from the clamps that affect the true force/distance measurements to the point of tissue failure (tear). Different methods were attempted to hold the samples in a static position, but ultimately, the samples did not stay clamped for the test duration before tearing (or maximum tensile strength) in every test. Tests were not immediately excluded when the specimen slipped from the clamps or ruptured adjacent to the grips. Typical stress–strain curves have a nonlinear character; 4 basic regions can be distinguished related to the distinct behavior of collagen fibers transmitting the mechanical

load, which were shown on our curves. However, having the ability to test the samples to the point of biomechanical failure would have been beneficial.

Another study limitation was the inclusion of heterogeneous tissue, harvested dogs varying in age, sex, and nutritional status and breed. Although care was taken to harvest from similar sites, anatomical and histological variations were noted, particularly regarding the harvested sample thickness, the amount of connective tissue, and fat thickness for each animal. The variability of donor animals, however, reflect the variability expected in patients needing expansion of tissue appears to be the best model based on the biomechanical and practical considerations.¹⁹

This study showed that the scalp was more receptive to the forces of expansion than the other sites. Tissue expansion is not without complications, and tissue acceptance of available devices must be considered before using this technique. The future goal of this research was to develop hydrogel tissue expanders specifically designed to exert forces and rates of expansion appropriate for specific anatomical sites.^{8,24} The data in this study provide initial values for these forces in devices for in vitro testing regarding ischemia and necrosis. Each uncontrolled expander may be formulated with the correct force of expansion for successful clinical use. Testing the biomechanical limitations of common sites of soft-tissue expansion warrants further investigation. Table 2 is definitions and descriptions of terms used.

Clark T. Barco, DDS, MS

Richard L. Roudebush VA Medical Center
Dental Service (160)
1481 West 10th Street
Indianapolis, IN 46202
E-mail: Clark.Barco@va.gov

ACKNOWLEDGMENTS

The content is solely the responsibility of the authors and does not necessarily represent the official views of the U.S. Department of Veterans Affairs, or the United States Government. Illustration

tions were prepared by Gudren Carlson from Medical Media Center at Roudebush VA Medical Center. The authors thank the staff of the Laboratory Animal Research Center at Indiana University, Indianapolis, Ind. for their dedication and help with the study; the Pathology Service, Roudebush VA Medical Center, Indianapolis, Ind., for providing histological laboratory for this study; Ms. Angela Skehan and Mr. Matthew Horn, Roudebush VA Medical Center, Indianapolis, Dental Service, for their help with article preparation; and Mr. John Garner, Manager, Akina, Inc. for his excellent advice. Indiana Institute for Medical Research (IIMR) is a nonprofit foundation that works to support and enhance research and development focused on improving the health and quality of life for our nation's Veterans and citizens. The authors acknowledge IIMR's support of the work described in this document. The authors thank the IIMR for support provided to conduct this study. Finally, the authors thank Texture Technologies and Mr. Wassilak for his aid in developing the testing methods and providing resources for utilization of the testing equipment.

REFERENCES

- Burkhardt R, Lang NP. Role of flap tension in primary wound closure of mucoperiosteal flaps: a prospective cohort study. *Clin Oral Implants Res.* 2010;21:50–54.
- Greenstein G, Greenstein B, Cavallaro J, et al. Flap advancement: practical techniques to attain tension-free primary closure. *J Periodontol.* 2009;80:4–15.
- Cordaro L, Amadé DS, Cordaro M. Clinical results of alveolar ridge augmentation with mandibular block bone grafts in partially edentulous patients prior to implant placement. *Clin Oral Implants Res.* 2002;13:103–111.
- Wang HL, Boyapati L. "PASS" principles for predictable bone regeneration. *Implant Dent.* 2006;15:8–17.
- Asa'ad F, Rasperini G, Pagni G, et al. Pre-augmentation soft tissue expansion: an overview. *Clin Oral Implants Res.* 2016;27:505–522.
- Cherry GW, Austad E, Pasyk K, et al. Increased survival and vascularity of random-pattern skin flaps elevated in controlled, expanded skin. *Plast Reconstr Surg.* 1983;72:680–687.
- Saulis AS, Lautenschlager EP, Mustoe TA. Biomechanical and viscoelastic properties of skin, SMAS, and composite flaps as they pertain to rhytidectomy. *Plast Reconstr Surg.* 2002;110:590–598; discussion 599.
- Barwinska D, Garner J, Davidson DD, et al. Mucosal perfusion preservation by a novel shapeable tissue expander for oral reconstruction. *Plast Reconstr Surg Glob Open.* 2017;5:e1449.
- Griffin M, Hindocha S, Malahias M, et al. Flap decisions and options in soft tissue coverage of the upper limb. *Open Orthop J.* 2014;8:409–414.
- Urban IA, Monje A, Nevins M, et al. Surgical management of significant maxillary anterior vertical ridge defects. *Int J Periodontics Restorative Dent.* 2016;36:329–337.
- Dahlin C, Linde A, Gottlow J, et al. Healing of bone defects by guided tissue regeneration. *Plast Reconstr Surg.* 1988;81:672–676.
- Kaner D, Friedmann A. Soft tissue expansion with self-filling osmotic tissue expanders before vertical ridge augmentation: a proof of principle study. *J Clin Periodontol.* 2011;38:95–101.
- Park JC, Kim CS, Choi SH, et al. Flap extension attained by vertical and periosteal-releasing incisions: a prospective cohort study. *Clin Oral Implants Res.* 2012;23:993–998.
- Corban J, Shash H, Safran T, et al. A systematic review of complications associated with direct implants vs. tissue expanders following Wise pattern skin-sparing mastectomy. *J Plast Reconstr Aesthet Surg.* 2017;70:1191–1199.
- Wiese KG. Osmotically induced tissue expansion with hydrogels: a new dimension in tissue expansion? A preliminary report. *J Craniomaxillofac Surg.* 1993;21:309–313.
- Rees L, Morris P, Hall P. Osmotic tissue expanders in cleft lip and palate surgery: a cautionary tale. *J Plast Reconstr Aesthet Surg.* 2008;61:119–120.
- Duquenois-Martinot V, Depoortere C, Deveaux C, et al. Indications de l'expansion chez l'enfant. Experience de 30ans d'activite et revue de la litterature. [Indications of the expansion in pediatric surgery. Experience of 30 years and literature review]. *Ann Chir Plast Esthet.* 2016;61:740–749.
- Held M, Engelke AS, Tolzmann DS, et al. Biomechanical skin property evaluation for wounds treated with synthetic and bio-synthetic wound dressings and a newly developed collagen matrix during healing of superficial skin defects in a rat models. *Wounds.* 2016;28:334–340.
- Bartell TH, Mustoe TA. Animal models of human tissue expansion. *Plast Reconstr Surg.* 1989;83:681–686.
- Wysocki M, Kobus K, Szotek S, et al. Biomechanical effect of rapid mucoperiosteal palatal tissue expansion with the use of osmotic expanders. *J Biomech.* 2011;44:1313–1320.
- Affolter VK, Moore PF. Histologic features of normal canine and feline skin. *Clin Dermatol.* 1994;12:491–497.
- Ohman C, Baleani M, Viceconti M. Repeatability of experimental procedures to determine mechanical behaviour of ligaments. *Acta Bioeng Biomech.* 2009;11:19–23.
- Cheng S, Gandevia SC, Green M, et al. Viscoelastic properties of the tongue and soft palate using MR elastography. *J Biomech.* 2011;44:450–454.
- Garner J, Davidson D, Eckert GJ, et al. Reshapable polymeric hydrogel for controlled soft-tissue expansion: *in vitro* and *in vivo* evaluation. *J Control Release.* 2017;262:201–211.